NASA/CR—1999-209301

Heat Transfer on a Film-Cooled Rotating Blade

Vijay K. Garg
AYT Corporation, Brook Park, Ohio

July 1999

The NASA STI Program Office . . . in Profile

Since its founding, NASA has been dedicated to the advancement of aeronautics and space science. The NASA Scientific and Technical Information (STI) Program Office plays a key part in helping NASA maintain this important role.

The NASA STI Program Office is operated by Langley Research Center, the Lead Center for NASA's scientific and technical information. The NASA STI Program Office provides access to the NASA STI Database, the largest collection of aeronautical and space science STI in the world. The Program Office is also NASA's institutional mechanism for disseminating the results of its research and development activities. These results are published by NASA in the NASA STI Report Series, which includes the following report types:

- TECHNICAL PUBLICATION. Reports of completed research or a major significant phase of research that present the results of NASA programs and include extensive data or theoretical analysis. Includes compilations of significant scientific and technical data and information deemed to be of continuing reference value. NASA's counterpart of peer-reviewed formal professional papers but has less stringent limitations on manuscript length and extent of graphic presentations.

- TECHNICAL MEMORANDUM. Scientific and technical findings that are preliminary or of specialized interest, e.g., quick release reports, working papers, and bibliographies that contain minimal annotation. Does not contain extensive analysis.

- CONTRACTOR REPORT. Scientific and technical findings by NASA-sponsored contractors and grantees.

- CONFERENCE PUBLICATION. Collected papers from scientific and technical conferences, symposia, seminars, or other meetings sponsored or cosponsored by NASA.

- SPECIAL PUBLICATION. Scientific, technical, or historical information from NASA programs, projects, and missions, often concerned with subjects having substantial public interest.

- TECHNICAL TRANSLATION. English-language translations of foreign scientific and technical material pertinent to NASA's mission.

Specialized services that complement the STI Program Office's diverse offerings include creating custom thesauri, building customized data bases, organizing and publishing research results . . . even providing videos.

For more information about the NASA STI Program Office, see the following:

- Access the NASA STI Program Home Page at ***http://www.sti.nasa.gov***

- E-mail your question via the Internet to help@sti.nasa.gov

- Fax your question to the NASA Access Help Desk at (301) 621-0134

- Telephone the NASA Access Help Desk at (301) 621-0390

- Write to:
  NASA Access Help Desk
  NASA Center for AeroSpace Information
  7121 Standard Drive
  Hanover, MD 21076

NASA/CR—1999-209301

Heat Transfer on a Film-Cooled Rotating Blade

Vijay K. Garg
AYT Corporation, Brook Park, Ohio

Prepared for the
Turbo Expo '99
sponsored by the American Society of Mechanical Engineers
Indianapolis, Indiana, June 7–10, 1999

Prepared under Contract NAS3–98106

National Aeronautics and
Space Administration

Glenn Research Center

July 1999

Acknowledgments

The author wishes to thank Dr. Raymond Gaugler, Chief, Turbine Branch, Mr. John Rohde of the Subsonic Systems Office, and Mr. K.C. Civinskas, Turbine and Combustor Technology Program Manager at the NASA Glenn Research Center, and Mr. Milt Ortiz of AlliedSignal Engines for their support of this work. Geometric and other details for the blade obtained from D. Yong Kim and Dr. Jong Liu of AlliedSignal Engines are also acknowledged.

Available from

NASA Center for Aerospace Information
7121 Standard Drive
Hanover, MD 21076
Price Code: A03

National Technical Information Service
5285 Port Royal Road
Springfield, VA 22100
Price Code: A03

HEAT TRANSFER ON A FILM-COOLED ROTATING BLADE

Vijay K. Garg
AYT Corporation
Brook Park, OH 44142
Mail Stop 5-11
Tel. (216) 433-6788; Fax (216) 433-5802
e-mail: vijay.garg@grc.nasa.gov

ABSTRACT

A multi-block, three-dimensional Navier-Stokes code has been used to compute heat transfer coefficient on the blade, hub and shroud for a rotating high-pressure turbine blade with 172 film-cooling holes in eight rows. Film cooling effectiveness is also computed on the adiabatic blade. Wilcox's k-ω model is used for modeling the turbulence. Of the eight rows of holes, three are staggered on the shower-head with compound-angled holes. With so many holes on the blade it was somewhat of a challenge to get a good quality grid on and around the blade and in the tip clearance region. The final multi-block grid consists of 4784 elementary blocks which were merged into 276 super blocks. The viscous grid has over 2.2 million cells. Each hole exit, in its true oval shape, has 80 cells within it so that coolant velocity, temperature, k and ω distributions can be specified at these hole exits. It is found that for the given parameters, heat transfer coefficient on the cooled, isothermal blade is highest in the leading edge region and in the tip region. Also, the effectiveness over the cooled, adiabatic blade is the lowest in these regions. Results for an uncooled blade are also shown, providing a direct comparison with those for the cooled blade. Also, the heat transfer coefficient is much higher on the shroud as compared to that on the hub for both the cooled and the uncooled cases.

NOMENCLATURE

B_p	blowing parameter {= $(\rho_c V_c)/[\rho_o (RT_o)^{1/2}]$}
d	coolant hole diameter
h	heat transfer coefficient (in W/m^2-K) based on $(T_{o,rel} - T_w)$
k	turbulence kinetic energy
ℓ	turbulence length scale
m	mass flow rate
m_o	mainstream mass flow rate
p	pressure
Pr	Prandtl number
R	gas constant
Re	Reynolds number
s	distance from the leading edge along the pressure (s < 0) or suction surface (s > 0) normalized by blade span at the trailing edge
T	temperature
Tu	turbulence intensity
v^*	shear velocity
V_c	average coolant velocity at the hole exit
x,y,z	Cartesian coordinate system with z-coordinate along the span
y^+	distance in wall coordinates (= yv^*/ν)
z_n	= (z - z for hub at trailing edge)/blade span at trailing edge
α	thermal diffusivity
Δy	distance (from the wall) of the first point off the wall
ε	turbulence dissipation rate
η	film cooling effectiveness [= $(T_{o,rel} - T_{aw})/(T_{o,rel} - T_c)$]
μ	viscosity
ν	kinematic viscosity
ρ	density
ω	specific turbulence dissipation rate (= ε/k)
Ω	rotational speed of the blade

Subscripts

aw	corresponding to adiabatic condition
c	for coolant (average value)
ef	effective value
ex	value at exit
in	value at inlet
ℓ	laminar value
o	stagnation value
rel	value relative to blade
T	turbulent value
w	value at wall

INTRODUCTION

It is well known from the thermodynamic analysis that the performance of a gas turbine engine is strongly influenced by the temperature at the inlet to the turbine. There is thus a growing tendency to use higher turbine inlet temperatures, implying increasing heat loads to the engine components. Modern gas turbine engines are designed to operate at inlet temperatures of 1800-2000 K, which are far beyond the allowable metal temperatures. Thus, to maintain acceptable life and safety standards, the structural elements need to be protected against the severe thermal environment. This calls for an efficient cooling system. One such cooling technique currently used for high

temperature turbines is film cooling. In this technique, cooler air is injected into the high temperature boundary layer on the blade surface. Since the injected cooler air is bled directly from the compressor before it passes through the combustion chamber, it represents a loss in the total power output. The designer's goal is therefore to minimize the amount of coolant necessary to insure adequate engine life. Unfortunately, the thermal design of a film-cooled blade is still based on one-dimensional analysis and empirical correlations, thereby requiring actual testing of every design concept. In such a situation, only minor variations of existing designs are adopted since any novel ideas are too expensive to test thoroughly. There is thus an urgent need to be able to predict accurately the heat transfer characteristics of film-cooled blades before actually testing them in the engine.

A considerable effort has been devoted to understanding the coolant film behavior and its interaction with the mainstream flow. The film cooling performance is influenced by the wall curvature, three-dimensional external flow structure, free-stream turbulence, compressibility, flow unsteadiness, the hole size, shape and location, and the angle of injection. Interest in this field has grown considerably in recent years. However, many studies on film cooling have been confined to simple geometries, for example, two-dimensional flat and curved plates in steady, incompressible flow.

An excellent survey of the film-cooling work up to 1971 has been provided by Goldstein (1971). Several further studies in this field have been summarized by Garg and Gaugler (1993, 1994, 1996). A number of parametric studies have been performed by Garg and co-workers to determine the effect of several parameters, such as the effect of coolant velocity and temperature distributions at the hole exit (Garg and Gaugler, 1997b), the effect of blade rotation and of the direction of coolant injection from the shower-head holes (Garg, 1997), the effect of spanwise pitch of shower-head holes (Garg and Gaugler, 1996), the effect of coolant to mainstream mass flow and temperature ratio (Garg and Gaugler, 1997a), and the effect of turbulence modeling (Garg and Abhari, 1997; Garg and Ameri, 1997; Garg, 1998, 1999). Four turbulence models, the Baldwin-Lomax model, Coakley's q-ω model, Chien's k-ε model, and Wilcox's *k*-ω models have been analyzed, and results compared with the experimental data for heat transfer from rotating as well as stationary blades. In all these studies by Garg and co-workers, coolant velocity and temperature distributions were prescribed at the hole exits. Moreover, while the true hole-exit on the blade surface is oval-shaped, it was approximated by a rectangle with steps owing to the use of a single-block grid. A recent study by Garg and Rigby (1999) analyzed in detail the coolant flow structure issuing out of compound-angled shower-head holes on a real blade. This study also presented an extensive survey of existing literature on the coolant flow characteristics at the exit of film-cooling holes.

We utilize the results of Garg and Rigby (1999) in studying the heat transfer characteristics of a three-dimensional high-pressure turbine rotor with 172 film cooling holes in 8 rows. We generate a multi-block grid that does not extend into the cooling hole pipes since there are too many (172) pipes. However, we retain the true shape of the hole exits on the blade surface, and pack as many as 80 control volumes within each tiny hole exit. Then we prescribe polynomial velocity and temperature distributions for the coolant flow at these hole exits. For the rotating case, the complete blade, the hub and the shroud with a tip clearance region are analyzed. Results for the heat transfer coefficient on the blade, hub and shroud corresponding to an isothermal condition, and for the film cooling effectiveness on an adiabatic blade are presented.

ANALYSIS

The numerical simulation has been performed using the NASA Glenn Research Center General Multi-Block Navier-Stokes Convective Heat Transfer code, Glenn-HT. Briefly, the code, formerly known as TRAF3D.MB (Steinthorsson et al., 1993, 1997), is an explicit, multigrid, cell-centered, finite volume code with a *k*-ω turbulence model without any wall functions. This is a general purpose flow solver designed for simulations of flows in complicated geometries. The Navier-Stokes equations in a rotating Cartesian coordinate system are mapped onto a general body-fitted coordinate system using standard techniques. The multistage Runge-Kutta scheme developed by Jameson et al. (1981) is used to advance the flow solution in time from an initial approximation to the steady state. A spatially varying time step along with a CFL number of 4 is used to speed convergence to the steady state. Eigenvalue-scaled artificial dissipation and variable-coefficient implicit residual smoothing are used along with a full-multigrid method. The overall accuracy of the code is second order. A single-block version of the same code, modified for film-cooling applications, was used by Garg and co-workers for the film cooling studies described earlier. The *k*-ω model of Wilcox (1994) with Menter's modifications (Menter, 1993) has yielded good results for heat transfer on film-cooled blades (Garg and Ameri, 1997; Garg, 1999), and is highly desirable for multi-block codes since it does not require the computation of distance from a wall. Also, no wall functions are used, thus avoiding any bias to the complex interactions between the coolant and the mainstream near the blade surface.

It is assumed that the effective viscosity for turbulent flows can be written as

$$\mu_{eff} = \mu_{\ell} + \mu_T$$

where the laminar viscosity μ_ℓ is calculated using a power-law for its dependence on temperature. The turbulent viscosity μ_T is computed using the low-Re *k*-ω model described by Rigby et al. (1996) and Ameri et al. (1997). The turbulent thermal diffusivity is computed from

$$\alpha_T = \frac{\mu_T}{\rho Pr_T}$$

where a constant value of 0.9 is used for the turbulent Prandtl number, Pr_T.

Boundary Conditions

At the main flow inlet boundary located at an axial distance approximately equal to the blade axial chord at mid-span upstream of the blade leading edge, the total temperature, total pressure, whirl, and meridional flow angle are specified, and the upstream-running Riemann invariant based on the total absolute velocity is calculated at the first interior point and extrapolated to the inlet. The velocity components are then decoupled algebraically, and the density is found from total temperature, total pressure and total velocity using an isentropic relation. For the turbulence model, the value of *k* and ω is specified using the experimental conditions, namely

$$k = 1.5\,(u_{in}\,Tu_{in})^2\ , \qquad \omega = k^{1/2}/\ell\ ,$$

where Tu_{in} is the intensity of turbulence at the inlet (taken to be 0.05), u_{in} is the inlet velocity, and ℓ is the turbulence length scale representing the size of the energy containing eddies. This length scale is usually not reported as part of the experimental conditions, and needs to be assumed. For the present study, ℓ was assumed to be 4% of the blade axial chord at mid-span. It may be noted that Garg and Ameri (1997) found negligible difference in the heat transfer coefficient at the surface of a film-cooled blade under similar mainstream conditions when Tu_{in} was raised to 0.15, and ℓ was taken to be 0.01 or 0.25 at the inlet, using the k-ε model. It is expected that a similar conclusion holds for the k-ω model for the present blade as well.

At the main flow exit plane located at an axial distance approximately equal to the blade axial chord at mid-span downstream of the blade trailing edge, the static pressure is specified and the density and velocity components are extrapolated from the interior. The local static pressure is found by integrating the axisymmetric radial equilibrium equation. At the solid surfaces of the rotating blade, hub and shroud, the no-slip condition is enforced, and either the isothermal (T_w/T_o = 0.646) or adiabatic condition is specified. The boundary conditions for turbulence quantities on the walls are k = 0, and

$$\omega = 100\,\frac{\partial u}{\partial y}\bigg|_{wall}$$

for a hydraulically smooth surface. An upper limit is imposed on the value of ω at the wall, as suggested by Menter (1993) and found effective by Chima (1996),

$$(\omega_{max})_{wall} = \frac{800}{Re}\,\frac{\nu}{(\Delta y)^2}$$

The grid around the blade extends to mid-way between two adjacent blades with periodic flow conditions in terms of cylindrical velocity components set on a dummy grid line outside this boundary. The boundary layer thickness on the hub and shroud was taken to be 7% of the blade span for the incoming flow to the rotor. The tip clearance region was handled by imposing periodicity conditions across the airfoil.

The effects of film cooling have been incorporated in the form of appropriate boundary conditions at the hole locations on the blade surface. Each hole exit in its true oval shape is represented by 80 control volumes. Different velocity and temperature profiles for the injected coolant can be specified at the hole exits. For the present results, polynomial distribution (Garg and Gaugler, 1997b) of coolant velocity (relative to the blade) and temperature at the hole exit was specified. Turbulent intensity at the hole exit was assumed to be 0.1, while the turbulence length scale at the hole exit was taken to be 0.25d. It has been reported by Garg (1999), however, that changing Tu to half the value and/or ℓ by a factor of 5 at the hole exit resulted in a negligible change in heat transfer coefficient at the surface of ACE rotor, except in the immediate vicinity of the holes. It is expected that a similar result would hold for the present rotor.

BLADE DETAILS

The present computation models an upcoming experiment to be performed at The Ohio State University, Columbus, Ohio, USA on an AlliedSignal film-cooled rotor. The turbine blade profile near mid-span along with the cooling row locations is shown in Fig. 1. There are 38 blades in the rotor. The number of holes in rows 1 through 8 are 32, 33, 16, 16, 16, 25, 17 and 17, respectively. The holes are all cylindrical with a diameter of 0.381 mm. Three rows (#3, 4, 5) are staggered with compound-angled holes on the shower-head. For these three rows, the hole angle with the spanwise direction varies from approximately 24° to 66°, and with the streamwise direction from 85° to 123°. For other rows of holes, the hole angle is 90° with the spanwise direction and varies from 24° to 45° with the streamwise direction.

COMPUTATIONAL DETAILS

The flow domain consists of the entire, three-dimensional, rotating blade with 172 film-cooling holes in 8 rows including three staggered rows of compound-angled shower-head holes, the hub, the shroud and the tip clearance region. The fact that the hole diameter is only 0.381 mm, about 1% of the blade axial chord at mid-span, and the tip clearance region is only about 1.3% of the blade span presents a challenge for grid generation. A multi-block grid is generated for the complex geometry using the commercial code GridPro/az3000 (Program Development Corporation, 1997). This consists of generating a system of locally structured grid blocks in a globally unstructured assembly. The grid generation code produces a body-fitted multi-block grid with hexahedral cells and full face-matching blocks.

Some details of the viscous grid are shown in Fig. 2. In this and Figs. 3 and 4, each elementary block is shown in a different color. The inviscid grid is first generated and the viscous grid is then obtained from the inviscid grid by clustering the grid near all the solid walls. The clustering is done in such a way as to ensure that in the viscous grid, the distance of any cell center adjacent to a solid wall, measured in wall units (y^+), is less than unity for the cases studied here, following Boyle and Giel (1992). Moreover, the clustered viscous grid near all wall boundaries does not extend into the far-flow field. Details of the grid on the blade pressure surface with several rows of holes are shown in Fig. 3. A blow-up of the grid near the shower-head hole exits as well as one row (#2) on the pressure surface is shown in Fig. 4. It may be noted that the exact oval shape of the hole opening on the blade surface is faithfully discretized. Also, the multi-block grid is able to transition smoothly from a very fine structure near locations of complex geometry such as hole boundaries to a coarse structure away from the holes. As can be observed from these figures, the grid quality is very good.

Initially, the grid consists of 4784 elementary blocks but before the solver is used, it can be merged into 276 super blocks using the Method of Weakest Descent (Rigby, 1996; Rigby et al., 1997). For so many super blocks, generation of the connectivity file and the data file for the application of boundary conditions was automated. There were a total of 1014 boundary condition patches on the blade surface, of which 514 were over the 172 hole exits and the remaining 500 on the blade solid surface. An additional 14 boundary condition patches covered the hub, the shroud, and inlet and exit for the main flow. In the above details, periodic boundary condition patches are not accounted for since the code takes care of periodicity via the connectivity data for the blocks.

The final viscous grid consists of a total of 2,205,760 cells, with 80 cells in each of the 172 hole exits. For computational accuracy the ratio of two adjacent grid sizes in any direction was kept within 0.8-1.25. We may point out that using the commercial code GridPro/az3000, two multi-block grids were first generated for the uncooled rotor for a grid independence study. One grid had twice as many cells in the streamwise direction as the other grid. The two grids yielded nearly identical heat transfer coefficient and pressure distributions at the blade surface. Computations were run on the 16-processor C90 supercomputer at NASA Ames Research Center. The code requires about 35 Mw of core storage with no blocks in the core memory, and another 450 Mw of scratch disk of which 295 Mw is configured for high speed I/O for reading and writing the blocks data. It takes about 110 s per iteration at the finest grid level. A case requires about 1500 iterations to converge.

RESULTS AND DISCUSSION

Results are presented for the heat transfer coefficient at the blade, hub and shroud surfaces for isothermal walls, and also for film cooling effectiveness on an adiabatic blade. Values for the various parameters for which the present simulation is performed are listed in Table 1, and the inlet angle for the main flow is shown in Fig. 5. It may be noted from Table 1 that the computed and given coolant mass flow ratios match very well. For the shower-head rows # 3, 4 and 5, the total coolant mass flow rate was given. While the computed total coolant mass flow for these rows is the same, it is instructive to look at the distribution which is like 4.8:1.7:1.0 through rows 3, 4 and 5. Values for the blowing parameter are also listed in Table 1. B_p varied from row to row except that it was the same for the shower-head rows 3, 4 and 5; also it was kept the same for all holes in a row.

Let us first look at the results for the uncooled rotor obtained by shutting off the coolant flow through the holes. Figure 6 shows the heat transfer coefficient, pressure and y^+ (for the first cell off the blade surface) distribution on the uncooled blade surface represented on the s-z_n plane, where s is the surface distance along the pressure or suction surface measured from the leading edge, and z_n is the z-coordinate measured from that for hub at the blade trailing edge, both normalized by the span at the trailing edge of the blade. Clearly, y^+ is less than 0.2 over the entire blade surface; this is in line with the requirement laid down by Boyle and Giel (1992) for accurate heat transfer prediction. We also note that the heat transfer coefficient is high in the leading edge region near the hub and all along the tip of the blade; it is also high on the suction surface near the tip just downstream of the leading edge. This is due to the flow crossing over from the pressure to the suction side through the tip clearance gap. For the distribution of main flow inlet angle as given in Fig. 5, the pressure is highest on the pressure side in the tip region just downstream of the leading edge.

Figure 7 shows the heat transfer coefficient, pressure and y^+ distribution on the hub and shroud corresponding to the uncooled blade case. Here again, y^+ is less than unity for the entire domain. The heat transfer coefficient is much higher on the shroud as compared to that on the hub. This is expected due to the tip clearance effect. From the pressure distribution, we note, similar to the observation for Fig. 6, that the main flow has a nearly zero incidence angle near the hub but impinges on the pressure side near the blade tip.

Figure 8 shows the streamlines, colored by static temperature, in the tip clearance region. The small inset shows the view looking on the blade tip directly from the top, while the larger view shows the tip vortices on the suction side of the blade clearly. The blade is shown in gray. The vortex in green is much stronger than that in blue which actually represents a half-turn (not visible in the figure). The streamlines do not show directly the cross-over of the mainstream flow from the pressure to the suction side through the tip clearance gap owing to the use of a tip clearance model. However, it was found later by gridding the tip clearance gap, thus avoiding use of any tip clearance model, that the heat transfer coefficient and effectiveness distributions on the blade surface changed very little from those presented here.

Figure 9 shows the heat transfer coefficient, pressure and y^+ (for the first cell off the blade surface) distribution on the isothermal, cooled blade surface represented on the s-z_n plane. A direct comparison between Figs. 6 and 9 reveals the differences between the uncooled and cooled blade surfaces. The heat transfer coefficient on the cooled blade surface is generally lower than that on the uncooled blade, except perhaps in the shower-head region and in the tip region on the suction side. Due to low coolant injection through the shower-head holes, the leading edge region has a high heat transfer coefficient even for the cooled blade. As is known, the pressure distribution is not much affected by film cooling. The y^+ distribution changes somewhat but y^+ values are still under 0.2 over the entire blade surface. Details of the heat transfer coefficient in the leading edge region are shown in Fig. 10 where rows #2 and 6 on the pressure and suction side are also shown along with the three staggered rows on the shower-head. Apparently, the region between rows 4 and 5 on the suction side has high heat transfer coefficient. This may be due to very low coolant mass flow rate through rows 4 and 5 (cf. Table 1). Also, the blade tip has high heat transfer coefficient. This may not be true for the real blade since the film cooling holes in the recessed tip were not included in the present study.

Figure 11 shows the heat transfer coefficient, pressure and y^+ distribution on the hub and shroud corresponding to the cooled blade case. Differences between the cooled and uncooled blade cases can be made by comparing Figs. 7 and 11. It may be noted that such differences are small. Thus, for the parameters of this study, film cooling does not affect the heat transfer coefficient and pressure distribution on the hub and shroud.

Figure 12 shows the film cooling effectiveness, pressure and y^+ distribution on the adiabatic blade surface represented by s-z_n coordinates. The effectiveness is the lowest in the leading edge region and near the tip, specially over the suction surface. Since h and η are both based on the difference from $T_{o,rel}$, it is natural to expect low values of η where h is high, and vice versa. The pressure and y^+ distributions are not much different from those in Fig. 9 for the isothermal, cooled blade. Figure 13 shows the details of film cooling effectiveness in the leading edge region near rows 2 through 6. The low effectiveness regions are clearly highlighted.

CONCLUSIONS

A multi-block, three-dimensional Navier-Stokes code has been used to compute heat transfer coefficient on the blade, hub and shroud

for a rotating high-pressure turbine blade with 172 film-cooling holes in eight rows. Film cooling effectiveness is also computed on the adiabatic blade. Wilcox's k-ω model is used for modeling the turbulence. It is found that for the given parameters, heat transfer coefficient on the cooled, isothermal blade is highest in the leading edge region and in the tip region. Also, the effectiveness over the cooled, adiabatic blade is the lowest in these regions. In the leading edge region, high values of h and low values of η are due to the rather low amount of coolant injected through the shower-head holes, while in the tip region, they are due to the mainstream flow crossing over from the pressure to the suction side through the tip clearance gap. Results for an uncooled blade are also shown, providing a direct comparison with those for the cooled blade. Also, the heat transfer coefficient is much higher on the shroud as compared to that on the hub for both the cooled and the uncooled cases, again due to the flow through the tip clearance gap.

REFERENCES

Ameri, A.A., Steinthorsson, E. and Rigby, D.L., 1997, Effect of Squealer Tip on Rotor Heat Transfer and Efficiency, ASME Paper 97-GT-128.

Boyle, R.J. and Giel, P., 1992, Three-Dimensional Navier Stokes Heat Transfer Predictions for Turbine Blade Rows, AIAA Paper 92-3068.

Chima, R.V., 1996, A *k*-ω Turbulence Model for Quasi-Three-Dimensional Turbomachinery Flows, AIAA Paper 96-0248.

Garg, V.K., 1997, Adiabatic Effectiveness and Heat Transfer Coefficient on a Film-Cooled Rotating Blade, *Numer. Heat Transfer, Part A*, Vol. 32, pp. 811-830.

Garg, V.K., 1998, Heat Transfer on a Film-Cooled Rotating Blade Using a Two-Equation Turbulence Model, *Int. J. Rotating Machinery*, Vol. 4, No. 3, pp. 201-216.

Garg, V.K., 1999, Heat Transfer on a Film-Cooled Rotating Blade Using Different Turbulence Models, *Int. J. Heat Mass Transfer*, Vol. 42, No. 5, pp. 789-802.

Garg, V.K. and Abhari, R.S., 1997, Comparison of Predicted and Experimental Nusselt Number for a Film-Cooled Rotating Blade, *Int. J. Heat & Fluid Flow*, Vol. 18, pp. 452-460.

Garg, V.K. and Ameri, A.A., 1997, Comparison of Two-Equation Turbulence Models for Prediction of Heat Transfer on Film-Cooled Turbine Blades, *Numer. Heat Transfer, Part A*, Vol. 32, pp. 347-371.

Garg, V.K. and Gaugler, R.E., 1993, Heat Transfer in Film-Cooled Turbine Blades, ASME Paper 93-GT-81.

Garg, V.K. and Gaugler, R.E., 1994, Prediction of Film Cooling on Gas Turbine Airfoils, ASME Paper 94-GT-16.

Garg, V.K. and Gaugler, R.E., 1996, Leading Edge Film Cooling Effects on Turbine Blade Heat Transfer, *Numer. Heat Transfer, Part A*, Vol. 30, pp. 165-187.

Garg, V.K. and Gaugler, R.E., 1997a, Effect of Coolant Temperature and Mass Flow on Film Cooling of Turbine Blades, *Int. J. Heat Mass Transfer*, Vol. 40, pp. 435-445.

Garg, V.K. and Gaugler, R.E., 1997b, Effect of Velocity and Temperature Distribution at the Hole Exit on Film Cooling of Turbine Blades, *J. Turbomachinery*, vol. 119, pp. 343-351.

Garg, V.K. and Rigby, D.L., 1999, Heat Transfer on a Film-Cooled Blade - Effect of Hole Physics, *Int. J. Heat & Fluid Flow*, Vol. 20, pp. 10-25.

Goldstein, R.J., 1971, Film Cooling, *Advances in Heat Transfer*, Vol. 7, pp. 321-379, Academic.

Jameson, A., Schmidt, W. and Turkel, E., 1981, Numerical Solutions of the Euler Equations by Finite Volume Methods Using Runge-Kutta Time-Stepping Schemes, AIAA Paper 81-1259.

Menter, F.R., 1993, Zonal Two-Equation *k*-ω Turbulence Models for Aerodynamic Flows, AIAA Paper 93-2906.

Program Development Corporation, 1997, "GridPro™/az3000 - User's Guide and Reference Manual," White Plains, NY.

Rigby, D.L., 1996, Method of Weakest Descent for Automatic Block Merging, Proc. 15th Intern. Conf. on Numer. Methods in Fluid Dynamics, Monterey, CA.

Rigby, D.L., Ameri, A.A. and Steinthorsson, E., 1996, Internal Passage Heat Transfer Prediction Using Multiblock Grids and a *k*-ω Turbulence Model, ASME Paper 96-GT-188.

Rigby, D.L., Steinthorsson, E. and Coirier, W.J., 1997, Automatic Block Merging Using the Method of Weakest Descent, AIAA Paper 97-0197.

Steinthorsson, E., Ameri, A.A. and Rigby, D.L., 1997, TRAF3D.MB - A Multi-Block Flow Solver for Turbomachinery Flows, AIAA Paper 97-0996.

Steinthorsson, E., Liou, M.S. and Povinelli, L.A., 1993, Development of an Explicit Multiblock/Multigrid Flow Solver for Viscous Flows in Complex Geometries, AIAA Paper 93-2380.

Wilcox, D.C., 1994, Simulation of Transition with a Two-Equation Turbulence Model, *AIAA J.*, Vol. 32, pp. 247-255.

Table 1 Parameter Values

p_o = 329.36 kPa; T_o = 460 K; T_c = 221.1 K
p_{ex} = 101.35 kPa; Ω = 11570.2 rpm; m_c/m_o = 0.0268
T_w = 297.2 K or $\partial T/\partial n = 0$ at blade and hub

row #	given m_c/m_o	computed m_c/m_o	B_p
1	0.47%	0.477%	0.3393
2	0.51%	0.508%	0.357
3	0.65%	0.419%	0.19
4		0.145%	0.19
5		0.086%	0.19
6	0.49%	0.493%	0.4528
7	0.35%	0.354%	0.4756
8	0.21%	0.214%	0.2854

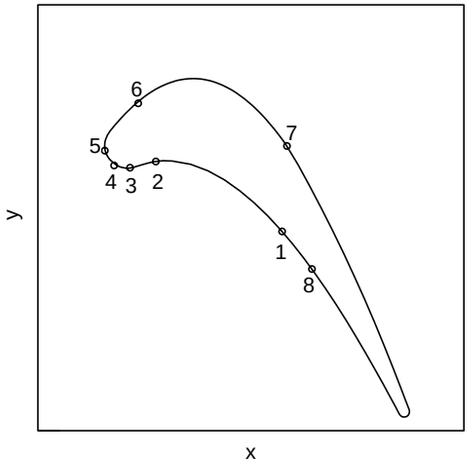

Fig. 1 Near mid−span profile of blade with hole−row locations

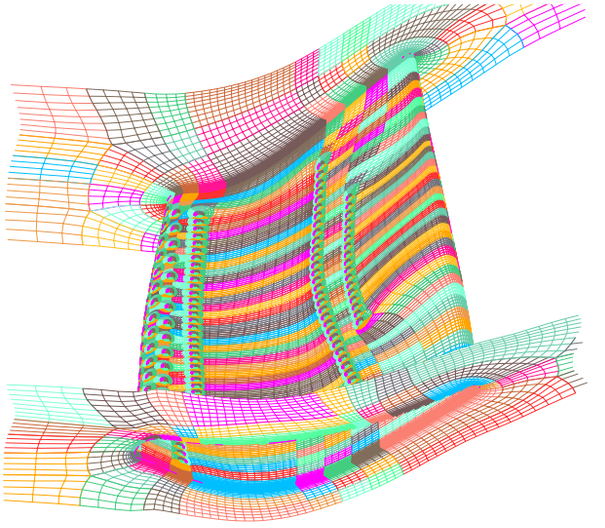

Fig. 2 Grid on hub, shroud and rotor with 172 film−cooling holes in 8 rows

Fig. 3 Grid on rotor pressure surface

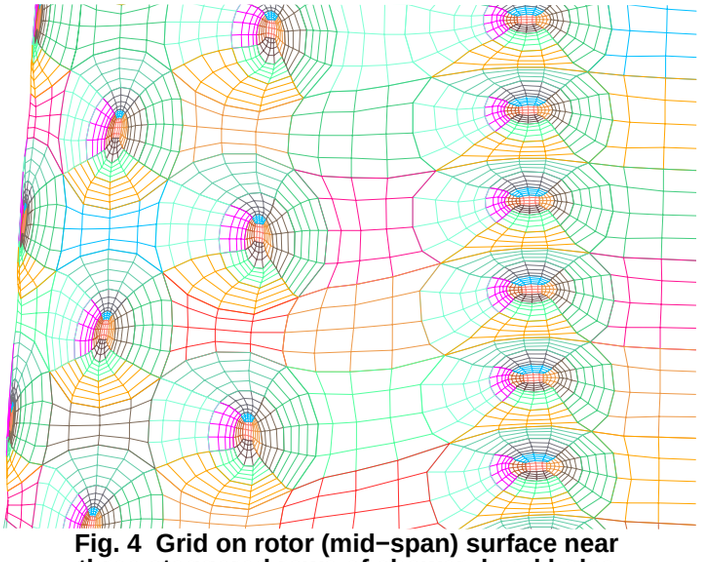

Fig. 4 Grid on rotor (mid−span) surface near three staggered rows of shower−head holes and row #2 on the pressure surface

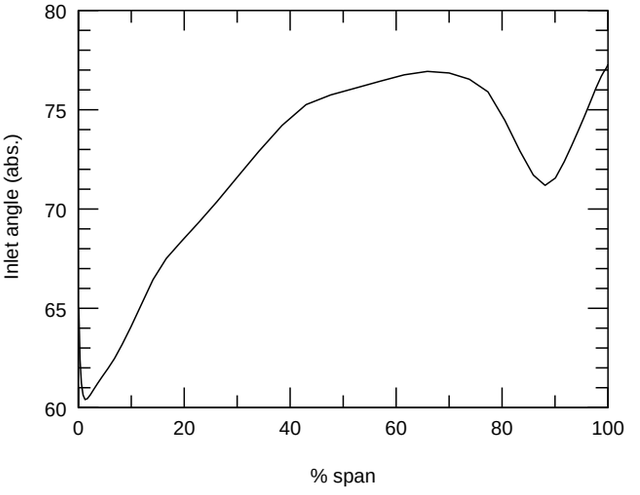

Fig. 5 Main flow angle at inlet to the rotor

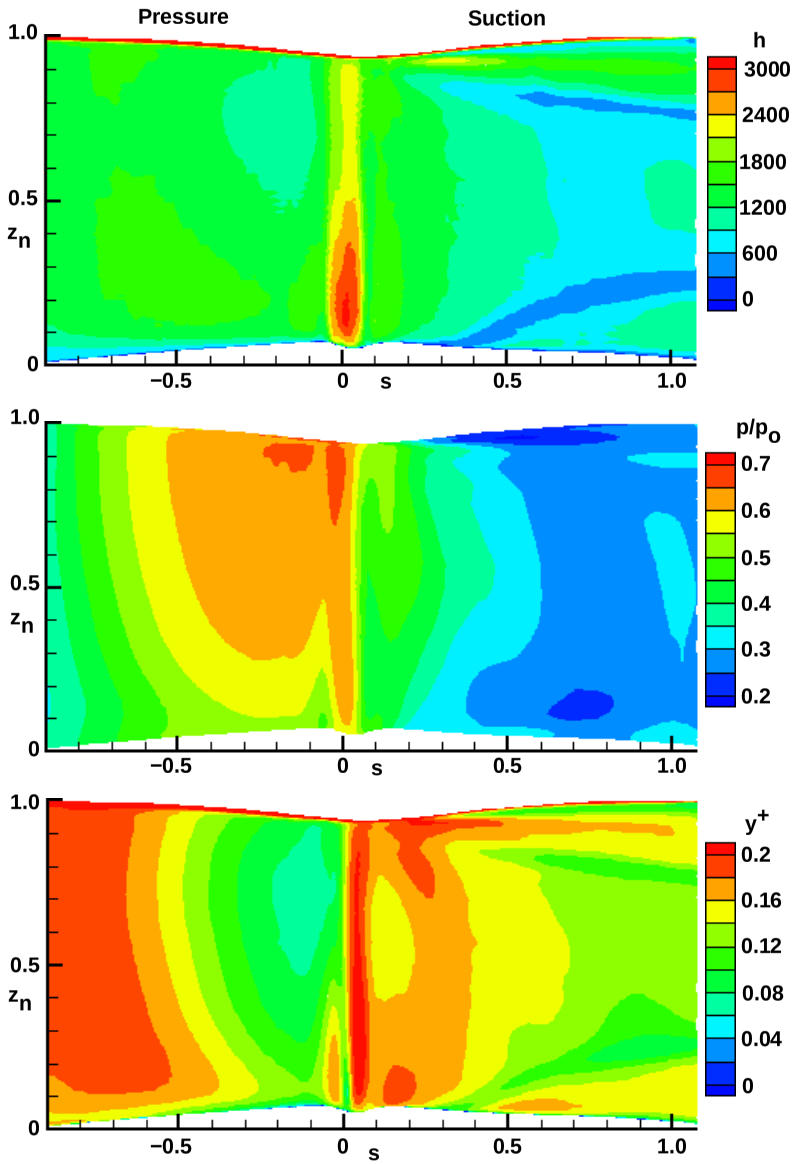

Fig. 6 Heat transfer coefficient, pressure and y^+ distribution on uncooled blade surface

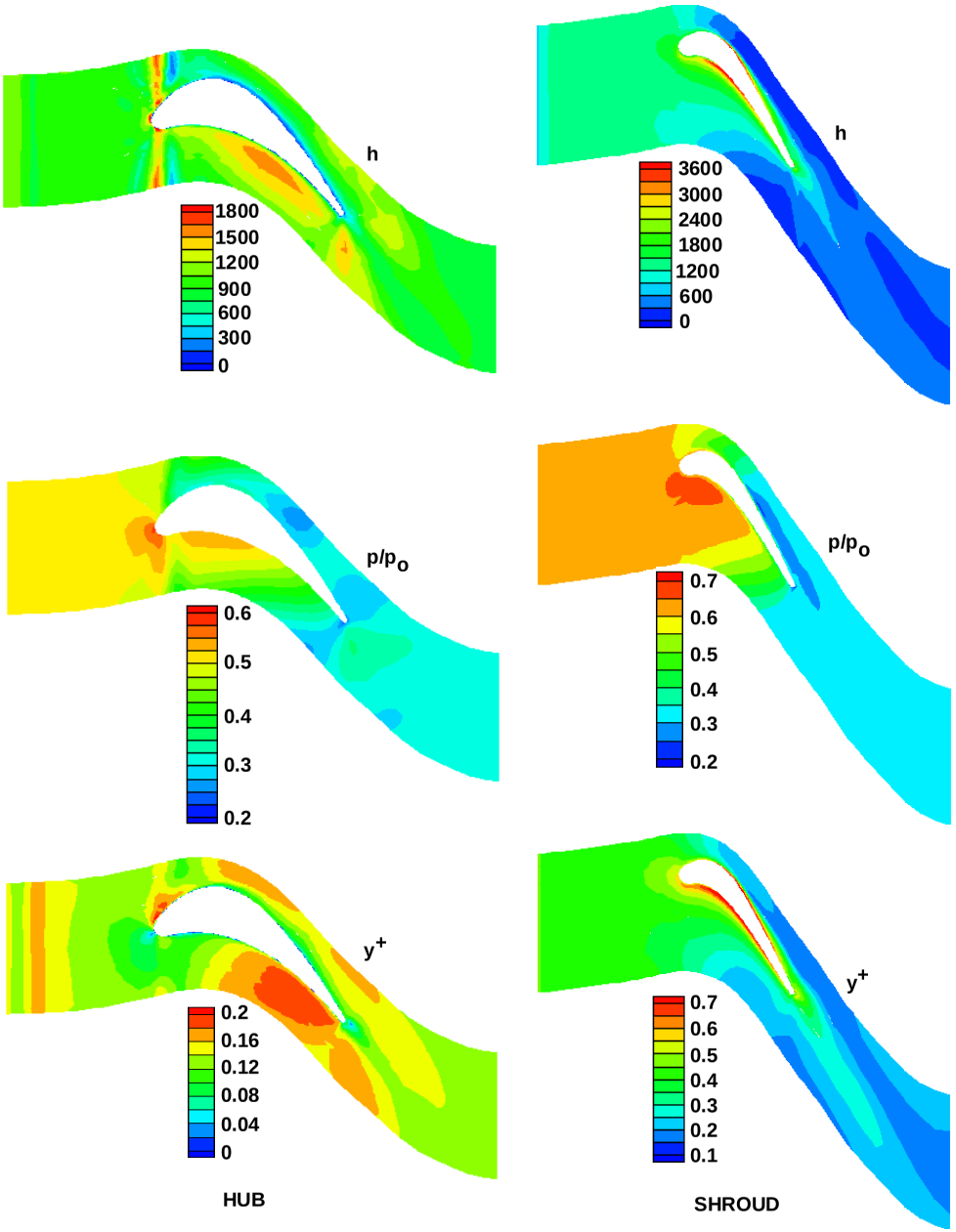

Fig. 7 Heat transfer coefficient, pressure and y^+ distribution on hub and shroud (uncooled rotor)

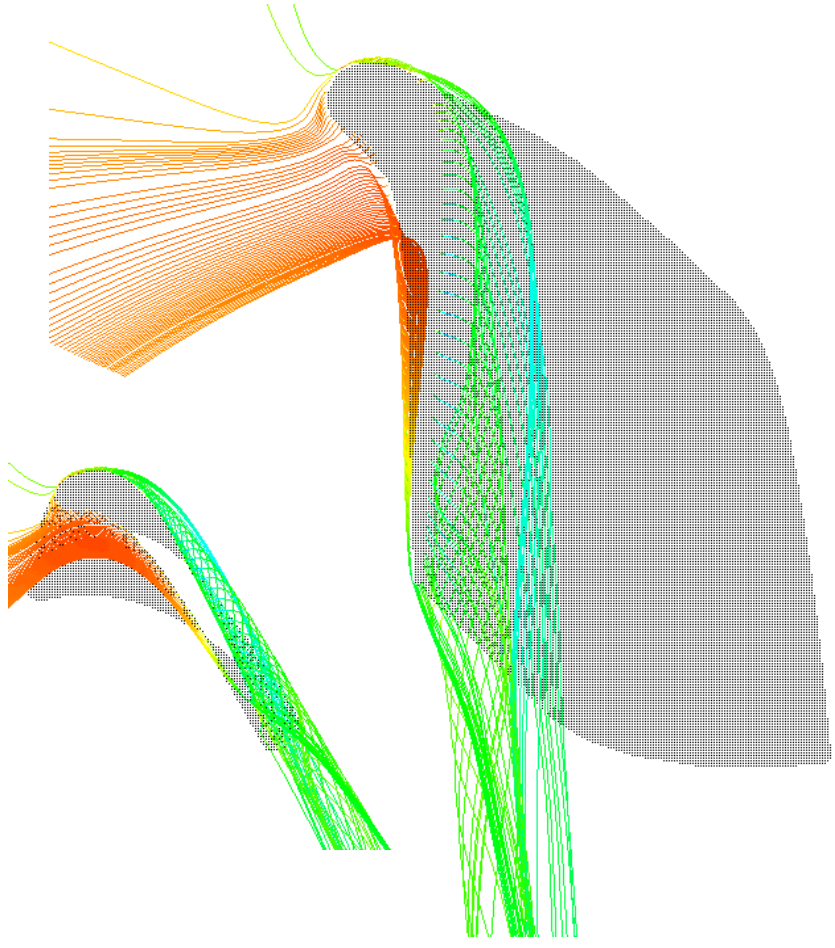

Fig. 8 Streamlines, colored by static temperature, in the tip−clearance region

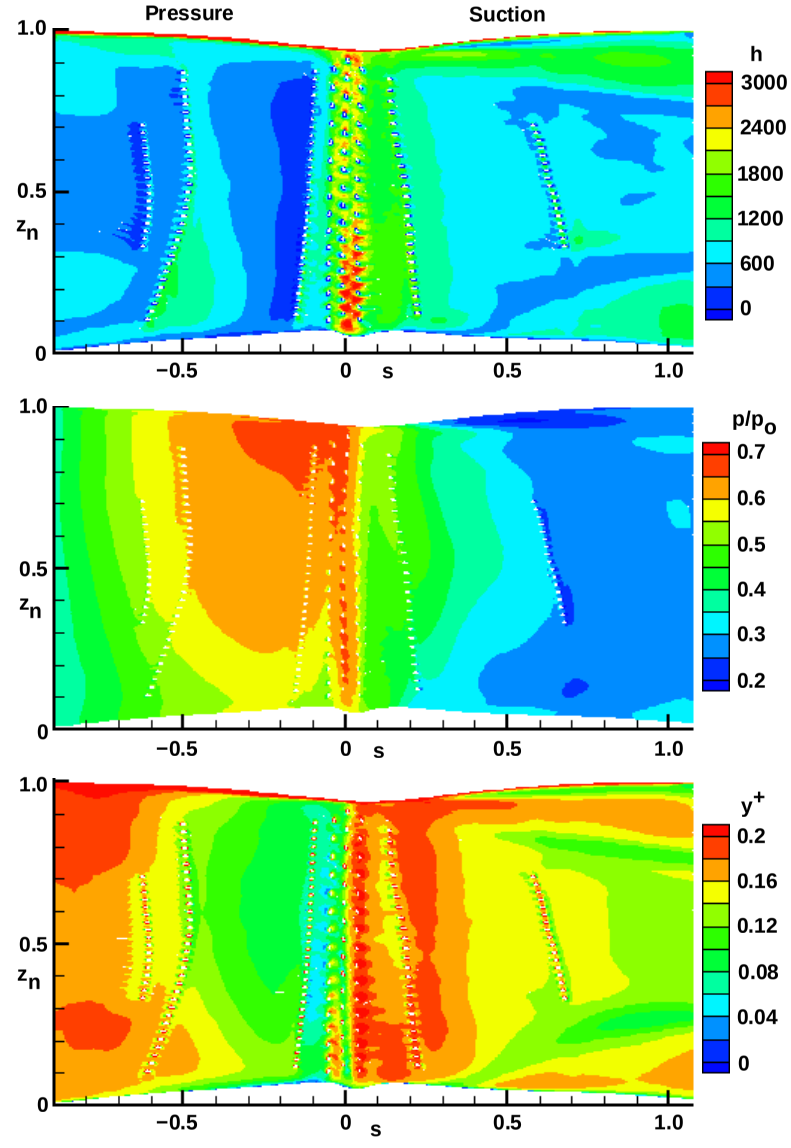

Fig. 9 Heat transfer coefficient, pressure and y^+ distribution on cooled blade surface

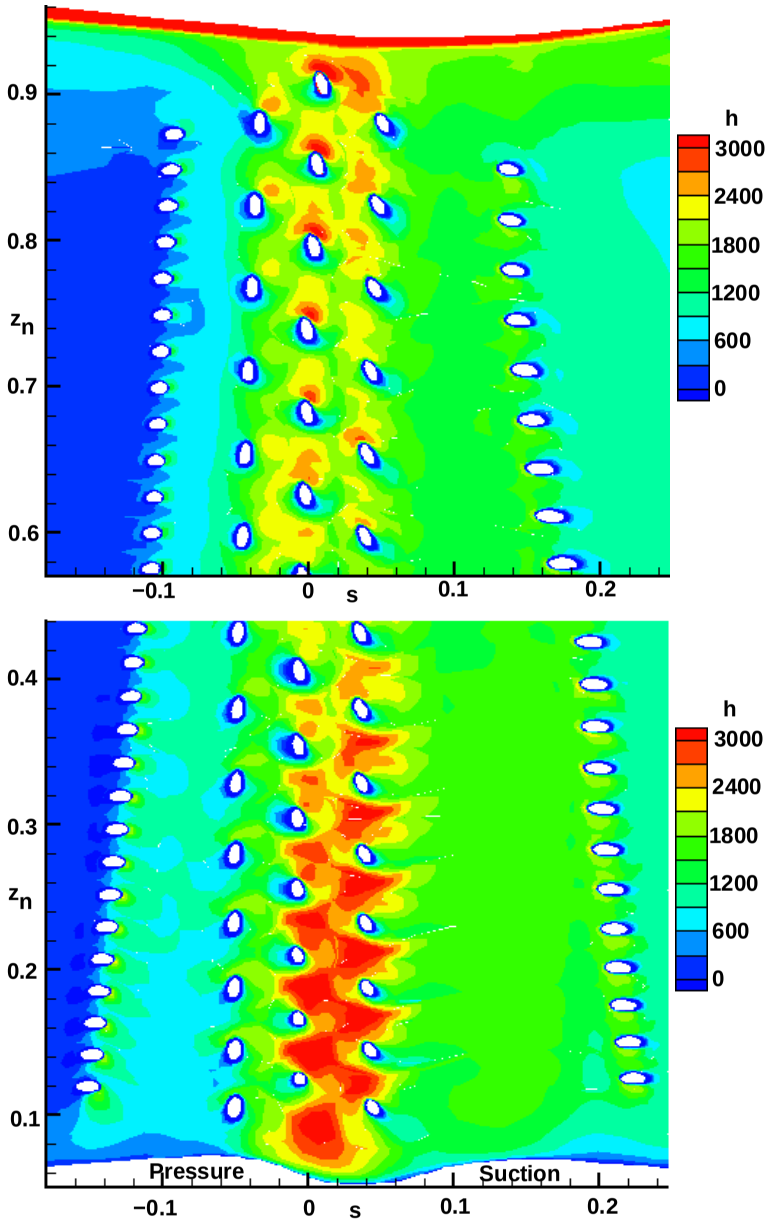

Fig. 10 Heat transfer coefficient in the leading edge region on cooled blade surface

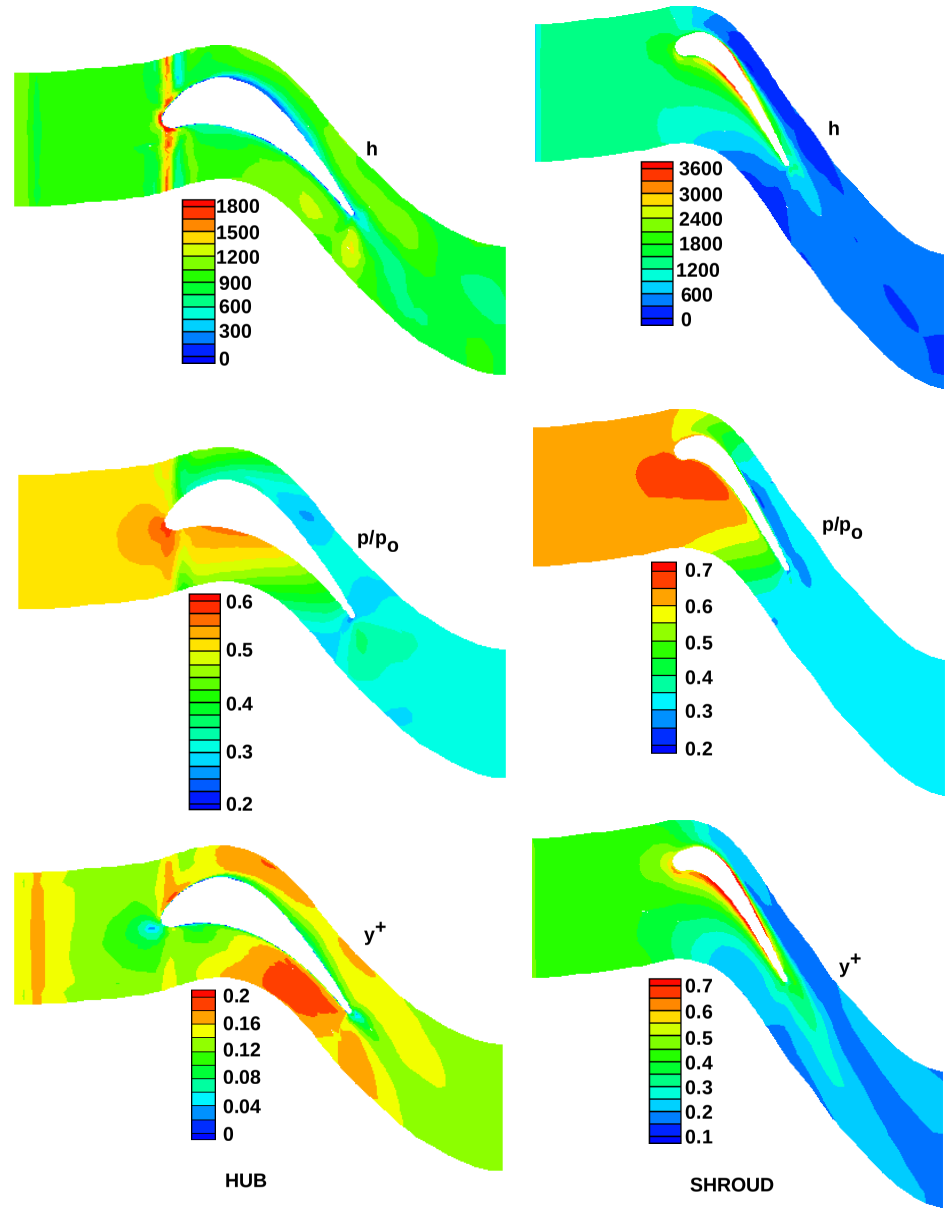

Fig. 11 Heat transfer coefficient, pressure and y^+ distribution on hub and shroud (cooled rotor)

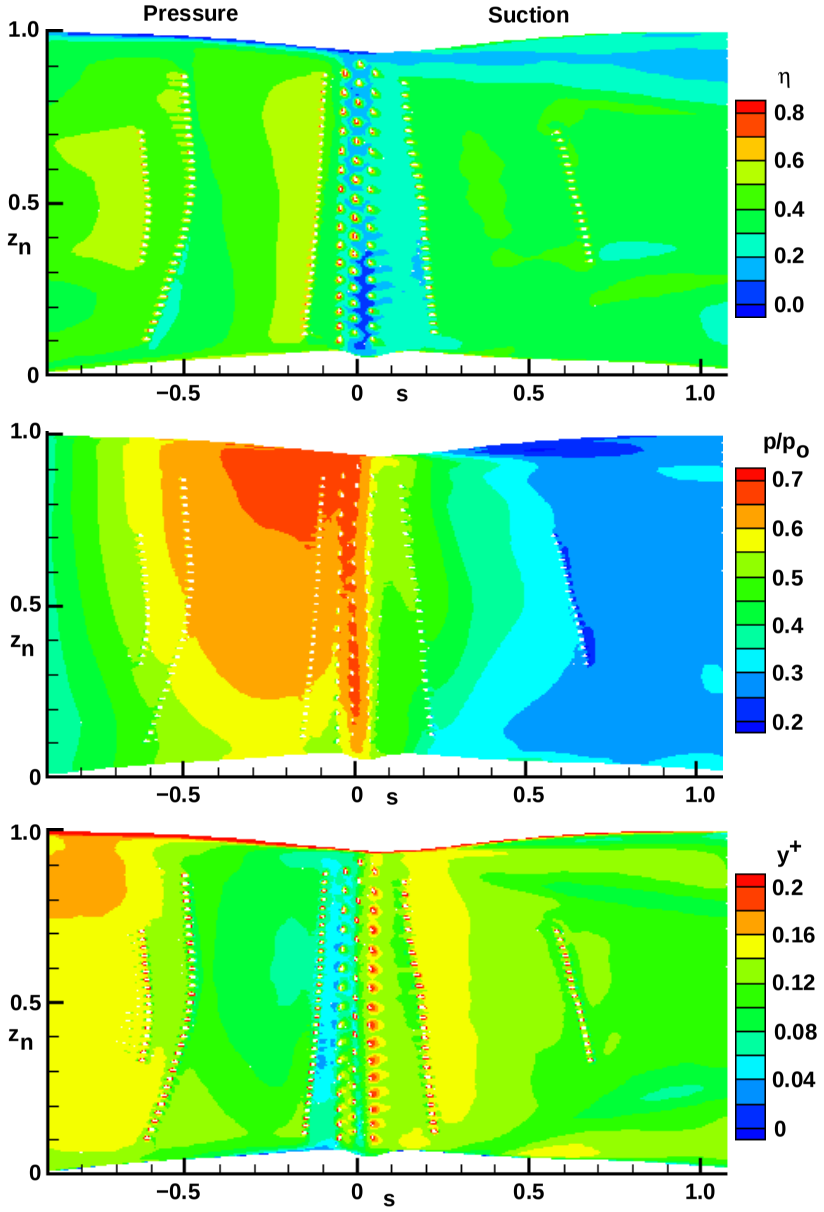

Fig. 12 Film cooling effectiveness, p/p_o and y^+ on the adiabatic blade surface

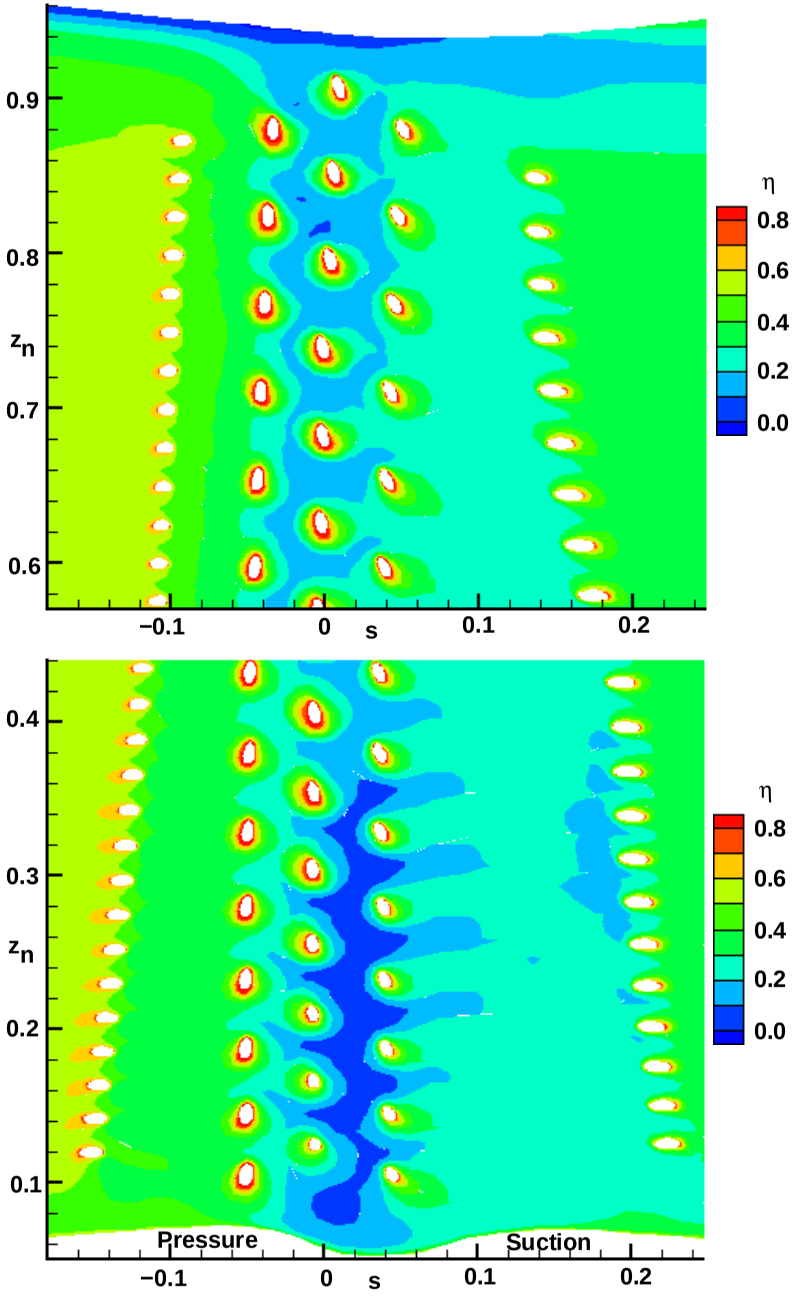

Fig. 13 Film cooling effectiveness in the leading edge region on the blade surface

REPORT DOCUMENTATION PAGE

Form Approved
OMB No. 0704-0188

1. AGENCY USE ONLY (*Leave blank*)	2. REPORT DATE	3. REPORT TYPE AND DATES COVERED
	July 1999	Final Contractor Report

4. TITLE AND SUBTITLE

Heat Transfer on a Film-Cooled Rotating Blade

5. FUNDING NUMBERS

WU–538–12–10–00
NAS3–98106

6. AUTHOR(S)

Vijay K. Garg

7. PERFORMING ORGANIZATION NAME(S) AND ADDRESS(ES)

AYT Corporation
Brook Park, Ohio 44142

8. PERFORMING ORGANIZATION REPORT NUMBER

E–11776

9. SPONSORING/MONITORING AGENCY NAME(S) AND ADDRESS(ES)

National Aeronautics and Space Administration
John H. Glenn Research Center at Lewis Field
Cleveland, Ohio 44135–3191

10. SPONSORING/MONITORING AGENCY REPORT NUMBER

NASA CR—1999-209301

11. SUPPLEMENTARY NOTES

Prepared for the Turbo Expo ‘99 sponsored by the American Society of Mechanical Engineers, Indianapolis, Indiana, June 7–10, 1999. Project Manager, R.E. Gaugler, Turbomachinery and Propulsion Systems Division, NASA Glenn Research Center, organization code 5820, (216) 433–5882.

12a. DISTRIBUTION/AVAILABILITY STATEMENT

Unclassified - Unlimited
Subject Categories: 02 and 34 Distribution: Nonstandard

This publication is available from the NASA Center for AeroSpace Information, (301) 621–0390.

12b. DISTRIBUTION CODE

13. ABSTRACT ***(Maximum 200 words)***

A multi-block, three-dimensional Navier-Stokes code has been used to compute heat transfer coefficient on the blade, hub and shroud for a rotating high-pressure turbine blade with 172 film-cooling holes in eight rows. Film cooling effectiveness is also computed on the adiabatic blade. Wilcox’s k-ω model is used for modeling the turbulence. Of the eight rows of holes, three are staggered on the shower-head with compound-angled holes. With so many holes on the blade it was somewhat of a challenge to get a good quality grid on and around the blade and in the tip clearance region. The final multi-block grid consists of 4784 elementary blocks which were merged into 276 super blocks. The viscous grid has over 2.2 million cells. Each hole exit, in its true oval shape, has 80 cells within it so that coolant velocity, temperature, k and ω distributions can be specified at these hole exits. It is found that for the given parameters, heat transfer coefficient on the cooled, isothermal blade is highest in the leading edge region and in the tip region. Also, the effectiveness over the cooled, adiabatic blade is the lowest in these regions. Results for an uncooled blade are also shown, providing a direct comparison with those for the cooled blade. Also, the heat transfer coefficient is much higher on the shroud as compared to that on the hub for both the cooled and the uncooled cases.

14. SUBJECT TERMS

Film cooling; Rotating blade

15. NUMBER OF PAGES

16

16. PRICE CODE

A03

17. SECURITY CLASSIFICATION OF REPORT	18. SECURITY CLASSIFICATION OF THIS PAGE	19. SECURITY CLASSIFICATION OF ABSTRACT	20. LIMITATION OF ABSTRACT
Unclassified	Unclassified	Unclassified	